# A THREE-DIMENSIONAL MODELING STUDY OF HAILSTORM SEEDING

Vlado Spiridonov[1] and Mladjen Curic[2]
[1]Hydrometeorological Institute, Skopje, Macedonia
[2] Institute of Meteorology, University of Belgrade, Serbia

Corresponding author address: Vlado Spiridonov
Hydrometeorological Institute, Skupi bb, 1000 Skopje, Macedonia

**Abstract**

A three-dimensional cloud model is used to simulate transport and diffusion of an artificial ice nucleation agent in conditions of hypothetical hailstorm seeding. The microphysical parameterization use the bulk a second-moment scheme for all species. According to the beneficial competition criteria silver iodide is directly injected and released into an assumed embryo formation region, between -8$^0$C and -12$^0$C isotherms and 25-45 dBZ radar reflectivity contours on line with length of 1.5 km.

The results from the case study simulation have shown that agent typically has about 2-3 min to spread in the seeding zone after its activation and relatively low vertical extension of spreading from the axis of dispersion, which is less than 160 m. The agent activation leads to earlier ice initiation that causes earlier initiation of precipitation.

The implication of the seeding is that cloud seeding with a 6 min time frequency contributes in registration of the maximum hailfall decrease at the ground of about 11.01 %, compared to the unseeded case.

The maximum rainfall increase of 25.79 % and hailfall decrease of 10% is found in the experiment with 0.4 g/m initial seeding rate, 5.5 km seeding height and 10 km seeding distance, compared to the base run simulation, respectively.

## 1. Introduction

Over the past two decades a number of papers have investigated the cloud seeding using numerical modeling. For example, Hsie et al., (1980), Curic and Janc, (1990, 1993), Curic et al., (1997), Farley et al. (1994, 2004) have revealed that the seeded cloud exhibits the earlier initiation of precipitation, with crucial seeding effects that lead to increased precipitation, slight dynamics and microphysics interactions and differences in cloud history. At the same time Orville et al. (1984) showed that some seeding treatments where resulted in a reduced precipitation, and Orville and Chen (1982) found reduced total precipitation for seeding. Farley (1987) found that hailfall decreased and rainfall could be increased in some situations, although some redistribution in hail spectrum can be expected. Orville et al., (1986) determine that seeding-induced glaciation of smaller developing cells may lead to earlier enhanced vertical growth due to the release of latent heat. The seeded large, vigorous cloud may produce less precipitation because of additional snow, particles, created by the cloud seeding, being transported rapidly to the anvil Orville et al. (1989). Aleksic et al., (1992) from their model simulation have found that only 2-3% of the target volume is actually being seeded. The most sensitive problem according to them is the limited spread of the seeding agent and the time available for the agent diffusion and activation.

Observational evidence for limited dispersion is presented by Huston et al., (1991), together with the modeling study. These aspects are also discussed by Dennis (1980), Warburton et al., (1986).

This study has been focused on two aspects: a three-dimensional simulation of agent transport, diffusion and activation during supercell storm seeding case and the effects obtained from a number of sensitivity experiments by using different initial seeding parameters. Finally the results are summarized and the principal conclusion of the seeding criteria is given.

## 2. Model

### *2.1. Model characteristics*

The present version of the model is a three-dimensional, nonhydrostatic, time- dependent, compressible system which is based on the Klemp and Wilhelmson [1978] dynamics, Lin et. al. [1983] microphysics, Orville and Kopp [1977] thermodynamics. The governing equations of the model include momentum conservation equations, thermodynamic and pressure equations, four continuity equations for the various water substances, a subgrid scale (SGS) turbulent kinetic energy equation (TKE) and continuity equations for chemical species associated with various cloud water species.

2.2. Microphysics parameterizations

For the parameterization of the microphysical processes we use the integrated (bulk) water parameterization by Lin et al., (1983) with significant improvement of hail growth parameterization. Instead of using the hail size spectrum from zero to infinity (idealized spectrum), Curic and Janc, [1995, 1997] proposed considering the hail size spectrum which includes only hail sized particles (larger than 0.5 cm in diameter; hereafter called realistic hail spectrum).

Seven different categories of the three phases of water have been considered in the model. Both bulk mass mixing ratios and number concentrations of cloud water, rainwater, cloud ice, snow, graupel and hail as well as the bulk mixing ratio of water vapor are also predicted in the model. Condensation and deposition of water vapor produce cloud water and cloud ice, respectively. Conversely, evaporation and sublimation of cloud water and cloud ice maintain saturation. Natural cloud ice is normally initiated by using a Fletcher-type equation for the ice nuclei number concentration. In this version of the model, cloud ice may also be produced by the Hallett-Mossop ice multiplication. Bergeron-Findeisen process transform some of the cloud water into cloud ice and to a certain extent both of them into snow. Rain is produced by the autoconversion of cloud water, melting of snow and hail, and shedding during the wet growth of hail. Hail is produced by autoconversion of snow, by the interaction of cloud ice and snow with rain and by immersion freezing of rain. Snow may be produced by autoconversion and the Bergeron-Findeisen growth of cloud ice and by the interaction of cloud ice and rain. All types of precipitation elements grow by different forms of accretion. Evaporation (sublimation) of all types of hydrometeors is also simulated.

Each of these number concentrations (N) or bulk mixing ratios (Q) has an equation with the following form::

$$\frac{\partial N}{\partial t}+\frac{\partial NU_j}{\partial x_j}-N\frac{\partial U_j}{\partial x_j}-\frac{1}{\rho}\frac{\partial \rho V_t N}{\partial x_3}=S+E_n \quad (1)$$

$$\frac{\partial Q}{\partial t}+\frac{\partial QU_j}{\partial x_j}-Q\frac{\partial U_j}{\partial x_j}-\frac{1}{\rho}\frac{\partial \rho V_t Q}{\partial x_3}=S+E_q \quad (2)$$

where S is the sink or source term, $V_t$ is the group terminal-falling-speed of any particular water category which was equal to zero for the cloud water and cloud ice in the model and $E_n$ or $E_q$ is the subgrid-scale contribution.

The equivalent radar reflectivity factors for hail and rain are computed using equations given by Smith et al., (1975) and empirical equation for snow by Sekhon and Srivastava (1970). More detail informations regarding the hydrodynamic equations, microphysics equations, turbulent closure and methods of solutions can be found in Telenta and Aleksic (1988) and Spiridonov and Curic (2003, 2005).

2.3. The calculation of agent dispersion

An additional conservation equation is considered here

$$\frac{\partial X_S}{\partial t}+\frac{\partial X_S U_j}{\partial x_j}-X_S\frac{\partial U_j}{\partial x_j}=S_{X_S}+E_{X_S} \quad (3)$$

where $X_S$ is the mixing ratio of AgI particles, $S_{X_S}$ is the sink or source term of mixing ratio and $E_{X_S}$ is the subgrid-scale contribution. The activation of AgI is parameterized by the three nucleation mechanisms based on Hsie (1980) and Kopp (1988) which are deposition (including sorption) nucleation, contact freezing nucleation – Brownian collection and inertial impact due to cloud droplets and raindrop. These are the sink terms of $X_S$ which can be calculated as:

1.) Contact freezing nucleation-Brownian collection, $S_{BC}$, and inertial impact due to cloud drops, $S_{IC}$,

$$S_{BC}=-4\pi D_S R_C X_S N_C \quad (4)$$

$$S_{IC}=-\pi {R_C}^2 X_S N_C V_C E_{CS}; \quad (5)$$

2.) Contact freezing nucleation-Brownian collection, $S_{BR}$, and inertial impact due to raindrops, $S_{IR}$,

$$S_{BR}=-2\pi D_S X_S N_{OR} \lambda_R^{-2} \quad (6)$$

$$S_{IR}=-2.54 E_{RS} \rho^{-0.375} X_S {q_R}^{0.875}; \quad (7)$$

3.) Deposition nucleation due to water vapor at ice supersaturation

$$S_{DN} = \begin{cases} m_s \dfrac{dN_{aD}(\Delta T)}{dt} & \text{when } 5°C \le \Delta T < 20°C \\ m_s N_{aD}(\Delta T) & \text{when } \Delta T \ge 20°C \end{cases} \quad (8)$$

where $D_S$ is a diameter of AgI particles, $N_C$ and $V_C$ the concentration and terminal velocity of cloud droplet, $R_C$ the cloud droplet radius, $N_{OR}$ parameter of the raindrop size distribution, $\lambda_R$ the slope parameter of rain, $E_{CS}$ and $E_{RS}$ are the collection efficiency of cloud water and rain water collecting AgI particles respectively, $\rho$ the air density, $N_{OR}$ the rainwater mixing ratio, $\Delta T$ supercooling and $N_{aD}$ is the number of AgI particles active as a deposition nuclei at a supercooling $\Delta T$, $m_s$ the mass of the AgI particle. These are the sink terms of $X_S$, while the initial mixing ratio $X_{S0}$ of agent homogeneously distributed in the seeding zone at the seeding moment is the source term of $X_S$.

An additional effort has been made in the study to consider the calculation of agent trajectories and its dispersion. In the rocket seeding, AgI is normally released as the line source with the length of 1 km, in a cylinder with a diameter of 10 m. Since the model dispersion of the agent is in its initial phase on a subgrid scale, the advection and diffusion should be parameterized. This problem is solved by considering the seeding line as a series of ten individual spherical puffs, each with a radius of 10 m. The agent spread is than simulated by the movement and spread of each individual puff. Its advection is calculated by a bilinear interpolation of the wind from the four adjacent grid points. The trajectories of the puffs are computed in the model. The radius $\sigma$ of these puffs has been calculated for each step as a function of the turbulent diffusion coefficient (Georgopoulos and Seinfeld, 1986) by the solution of the equation

$$\sigma_{i+1}^2 = \sigma_i^2 + 2K\Delta t \quad (9)$$

where K is the turbulent diffusion coefficient calculated using bilinear interpolation taken from the four adjacent points $\sigma_{i+1}$ is the radius of puff in time interval i+1 , $\sigma_i$ is the puff radius in the previous time step, and $\Delta t$ is the time step. The concentration of each puff is calculated by the following equation

$$C_{PUFF}(L) = \frac{4 \cdot Q_{PUFF}}{\pi \cdot D_{PUFF}(L)^2} \quad (10)$$

where L=1, LCS where LCS is the total number of puffs, $Q_{PUFF}$ is the seeding amount in g/m, and $D_{PUFF} = 2\sigma$ is the diameter of the puff. The initial AgI mixing ratio is then computed by the following term

$$X_{S0}(I0,J0,K0) = X_{S0}(I0,J0,K0) + C_{PUFF}(L) \quad (11)$$

Here, I0=INT(XPUFS)+1, J0=INT(YPUFS)+1, K0=INT(ZPUFS)+1 are the integer values of puffs coordinates in each direction x,y and z, respectively.

$$\begin{aligned} &XPUFS = XPUF(L)/H; \\ &YPUFS = YPUF(L)/H; \\ &ZPUFS = ZPUF(L)/D - 0.5 \end{aligned} \quad (12)$$

where

$$\begin{aligned} &XPUF(L) = XPUF(L) + UINT \cdot \Delta t; \\ &YPUF(L) = YPUF(L) + VINT \cdot \Delta t \\ &ZPUF(L) = ZPUF(L) + WINT \cdot \Delta t \end{aligned} \quad (13)$$

In the above terms XPUF(L), YPUF(L) and ZPUF(L) are the corresponding dimensions of puffs, H is the horizontal grid step, D is the vertical grid step and UINT, VINT and WINT are the bilinearly interpolated velocity components.

*2.4. Numerical technique*

Model equations are solved on a semi staggered grid. All velocity components $u_i$ are defined at one-half grid interval $0.5\Delta x_i$ while scalar variables are defined at the mid point of each grid. All velocity components and the horizontal and vertical advection terms are calculated by the centered fourth-and second-order differences, respectively. Since the model equations are compressible, a time splitting procedure with second-order leapfrog scheme is used for the portions which do not involve sound waves to achieve numerical efficiency. Forward-backward time differencing scheme is used for the acoustic part of the equations. An Eulerian fourth order central difference advection scheme has been used to calculate the puff advection.

*2.5. Boundary conditions*

The normal component of the velocity is assumed to vanish along the top and bottom boundaries. In order to remove suspicions that the vertical oscillations in the numerical simulation are caused by the rigid top boundary in a model, the model is upgraded by a radiative upper boundary condition, according to suggestions given by Klemp and Duran, (1983). The lateral boundaries are opened and time-dependent, so that disturbances can pass through with minimal reflection. Two different cases with regard to the wind velocity are considered according to Durran (1981). When the component of velocity normal to the boundary is directed toward the domain (inflow boundary), normal derivatives are set to be zero.

*2.6. Initial conditions and initialization*

Initial impulse for convection is an ellipsoidal warm bubble with the maximum temperature perturbation in the bubble center ($T_0 = 2.5°C$). The model domain covers 20x20x15km with (0.5x0.5x0.25km) resolution for the first three-dimensional simulation and 30x30x15 km (1x1x0.5km) for the second run, respectively. The temporal resolution of the model for integration of the dynamics, microphysics and chemistry is 5 and 10 s, and a smaller one is 1 and 2 s, for solving the sound waves. A representative sounding taken at 01 UTC from Petrovec on May 18, 2003 with the corresponding wind profile is presented in Fig.1. The sounding is unstable and moist and the cloud develops very quickly in response to the initiating perturbation.

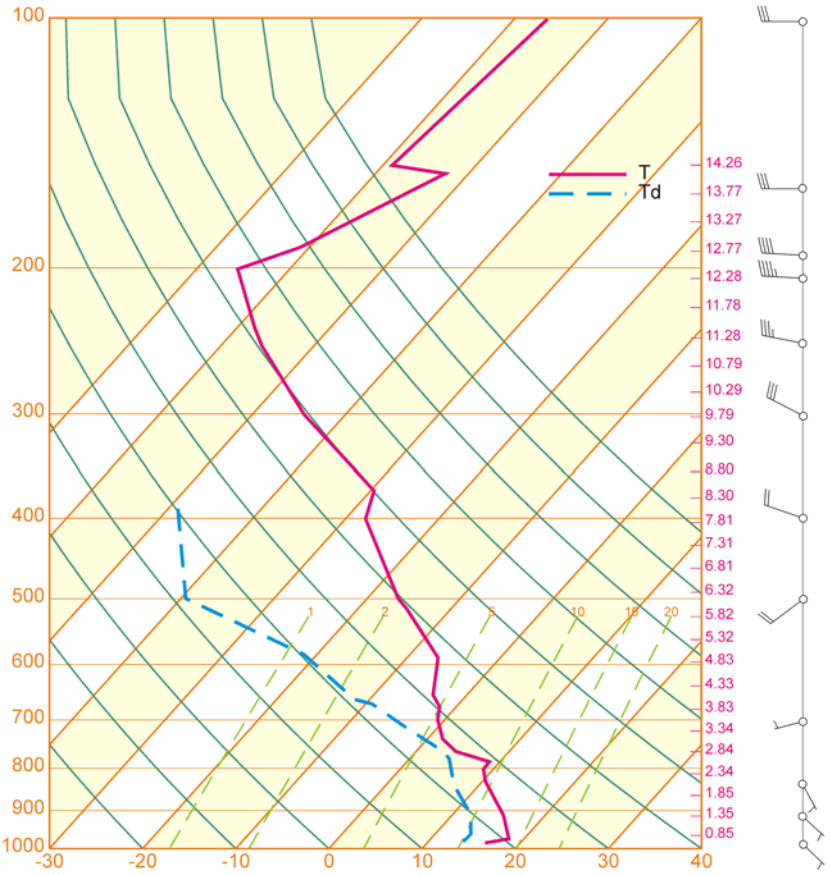


**Figure 1.** The 1200 UTC atmospheric sounding for Skopje, on May 18, 2003. Coordinate lines denote pressure (hPa) and temperature (°C). The solid line represents the temperature profile and the dashed line represents the moisture profile. Symbols on the r.h.s. of the same figure denote wind vectors (direction and velocity).

## 3. Results

### *3.1. A three-dimensional simulation of hailstorm seeding*

A three-dimensional simulation of the May 18 case indicates that the results are sensitive to the initial conditions. If it is sufficiently strong, the model cloud penetrates through the stable layer and then experiences explosive growth. Fig. 2a shows three-dimensional views of the cloud life cycle at 10-min intervals. The modeled cloud penetrates the stable layer and than experiences explosive growth, developing into vigorous storm, accompanied by the formation of large amount of ice phase particles. The mature phase of the storm appears after 30 min of the integration time when extensive precipitation occurs. The time evolution of AgI and (AgI+cloud) field at 1.6-min intervals starting at 23.3min, viewed from the southeast (SE) is depicted on Fig. 2b and Fig. 2c, respectively. According to the hail suppression method the silver iodide agent is directly injected into the simulated cloud in its developing stage at 5-min repeat seeding at 16.6 and 21.6 min, in the area between -8° C and -12°C isotherms and 25dBz-45dBz echo contours at 5.5 and 5 km height, respectively. The time evolution of the AgI field in the X-Z cross sections is depicted in Fig.3a. The AgI field is represented with an outer contour of 0.05 μg $kg^{-1}$ for 16.6 and 20.0 min and 0.015 μg $kg^{-1}$ contours for 23.3 min, with contour interval of 0.01μg $kg^{-1}$. After seeding the agent is advected and diffused within the cloud by the turbulent flow field. Some of the AgI has been activated; small part tends to be drawn back into the cloud as it descends to the lower levels by the downdrafts, while the large portion is transported outside the target volume above -12°C isotherm. The limited time spread of agent is may be due to the strong air circulation within the cloud. Only 9.6% of the AgI remains unactivated as a result of less than optimal placement of the seeding agent and the limited advection time of 2-3 min that limits the time available for agent diffusion. The maximum agent spread within the target area during simulation time is less than 90 m from the axis depending on the local turbulence. Fig. 3b shows the X-Y cross sections at z =5.5 km. The AgI boundary field and the contour interval are taken to be the 0.01μg $kg^{-1}$ contour. It is seen from this figure that after the seed was introduced into the target area the AgI is slowly diffused in response to the existing horizontal wind field at that level. The AgI mixing ratio decreases from 0.28 μg $kg^{-1}$ at 16.6 min to 0.065 μg $kg^{-1}$ at 26.6 min. Most of the AgI has been activated during the first five-minute interval. The unactivated AgI is initially transported toward southeast and downward. After repeat seeding two separated AgI fields are propagated and distributed toward eastern quadrant of the cloud model domain.

### *3.2. Evolution of physical and agent dispersion properties*

The most sensitive hailstorm seeding problem appears to be the limited spread of the seeding agent and limited time available for the agent diffusion and activation in the target volume. In order to gain a qualitative understanding of hailstorm seeding we investigate the seeding methods and conditions with varying assumptions regarding the seeding in order to determine optimal seeding parameters such as: seeding amount, time repetition of seeding, initial time of seeding, seeding height and distance. We have first investigated the influence of time interval of seeding on the total rainfall and hailfall on the ground.

Table 1 lists the parameters that distinguish ten numerical experiments using a second-moment model. The first run is chosen as a standard non-seeded case which serves as a basis for comparison with other experiments.

We compare rainfall and hailfall totals which were accumulated in the same total model integration time. The integration time was selected so that all precipitation were ended before the end of all simulations. It is evident that the total rainfall increases and hailfall decreases for all experiments relative to the base run case. One sees that the greatest rainfall increase of 25.79% is observed for a four-minute repeat of seeding for simulation A4. The experiment A1 indicates a peak rainfall increase of 6.23%. Hail amounts were much smaller but indicated decreases of 11.01% for case A7 and the minimum effect of seeding of 0.33% hailfall decrease is evidenced for run A1.

As is shown in Table 1 (columns, 3-7), most of the seeding agents act as deposition nuclei. In case A3 only 4.8% of the AgI particles remained unactivated. The seeding agent through inertial impact and Brownian collection by clouddrops and raindrops show very small effect on AgI activation. The next goals of this investigation is to examine the sensitivities of cloud seeding, including agent dispersion, to the physical processes which take place in-cloud and in the near cloud environment. As can be seen in Table 2, the maximum spread of the puff diameter within the target region is less than 90m, depending on the intensity of turbulence. The vertical extension

of the seeding zone depends on the regular placement of the seeding and the windflow within the cloud, and organization of its downdrafts and updrafts. One sees that the agent dose rate of 0.1 g/m contributes a larger vertical extent of the seeding zone of 87.6m. After seeding the AgI particles are advected and diffused within the cloud before the activation occurs. The artificial ice-phase particles produced by seeding lead to increase of the cloud ice mixing ratios relative to the unseeded case. The mixing ratios of other hydrometeors with except of snow slightly differ, comparing to those given from the base run simulation. It is also found that the seeding amount do not influence significantly on the total horizontally summed rainfall and hailfall on the ground in case of very large vigorous cloud. The seeding amount of about 0.4g/m, initial seeding time of 16.6min, on height 5.5km at distance of 10km in case B2 contribute in peak rainfall depth increase by about 25.79% and hailfall decrease of about 10.01 %.

These percentage numbers refer to the maximum rainfall increases calculated in the simulation time, after the initial cloud seeding. The effect of AgI seeding in respect to their microphysics is apparent if we consider the time evolution of reflectivity patterns of the unseeded and seeded cloud (Fig. 4). There is a slight similarity between the reflectivity echo contours after the initial seeding. The seeded case exhibits earlier development of precipitation and transformations in respects to its microphysics. The difference in the reflectivity echo fields between these runs becomes more evident as the cloud enters its mature stage. While the calculated reflectivity of the seeded case is within the range between 5 and 25 dBz at 60 min of the simulation, in the unseeded case the reflectivity zone with 35 dBz contour still exists.

## 4. Summary

According to hail suppression hypothesis it is logical to expect significant decrease of hail at the ground as in the other carefully setup hail suppression experiments. Despite positive statistical results from a number of numerical studies our sensitivity experiments indicate peak rainfall increased by about 25.79% and smaller hailfall decrease of 11.01%. This result may be due the limited spread of the seeding agent and the relatively low time of its diffusion and activation in the case of very large vigorous clouds. Numerical models should be enabling to correctly simulate the agent dispersion that is in its initial phase on a sub-grid scale. However, it is not possible easy to say that the seeding does not have any effects considering the differences especially in respect to their microphysics.

The results from the case study simulation have shown that agent typically has about 2-3 min to spread in the seeding zone after its activation and relatively low vertical extension of spreading from the axis of dispersion, which is less than 190 m. The agent activation leads to earlier ice initiation that causes hailstorm modification, earlier initiation of precipitation and difference in respect to microphysics, especially in cloud mature stage.

The implication of the seeding is that cloud seeding with 6 min time frequency contributes in registration of the maximum hailfall decrease at the ground of about 11.01 %, compared to the unseeded case. The maximum rainfall increases of 25.79 % and hailfall decreases of 10% is found in the experiment with initial seeding rate of 0.4 g/m, 5.5 km seeding height and 10 km seeding distance relative to base case.

***Acknowledgements.*** We would like gratefully to acknowledge to Dr. M. Gusev and Mr. B. Jakimovski from Institute of Informatics, University of Skopje for their help in preparing the 3-d plots.

***References***

Aleksic, N., B. Telenta and S. Petkovic, 1992: Model simulation of seeding repeat rates for direct injection seeding rockets. *J. Wea.Mod.,* **24**, 84-88.

Curic, M., and D. Janc, 1990: Numerical study of the cloud seeding effects. *Meteor. Atmos. Phys.,* **42**, 145-164.

Curic, M., and D. Janc, 1993: Dependence of the simulated seeding effects of Cb cloud on the types of the AgJ agents. *Meteor. Atmos. Phys.,* **52**, 145-164.

Curic, M., D. Janc, and V. Vuckovic, 1997: The influence of cloud drop size distribution on simulated seeding effects of hail-bearing cloud. *J. Wea. Mod.,* **29**, 70-73.

Curic, M., D. Janc, D. Vujovic and V. Vuckovic, 2003: The 3-D model characteristics of a Cb cloud which moves along a valley . *Meteor. Atmos. Phys.,* **84**, 171-184.

Dennis, A.,1980: Weather modification by cloud seeding. Academic Press, New York, 267 pp.

Durran, D.R., 1981: The effects of moisture on mountain lee waves. Ph.D. Thesis. Massachusetts Institute of Technology Boston, MA (NTIS PB 82126621).

Farley, R. D., 1987: Numerical modeling of hailstorms and hailstone growth. Part III: Simulation

of Alberta hailstorm-natural and seeded cases *J. Appl. Meteor*.,**26**,789-812.

Farley, R.D., P. Nguyen, and H.D. Orville, 1994: Numerical simulation of cloud seeding using a three-dimensional cloud model. *J. Wea.Mod*., **26,** 113-124.

Farley, R. D., T. Wu, H. D. Orville, and M. R. Hjelmfelt, 2004: Numerical simulation of hail formation in the 28 June 1989 Bismarck Thunderstorm: Part 1, Hail Growth. *Atmos. Research*, **71**, 51-79.

Farley, R.D., H. Chen, H.D. Orville and M.R. Hjelmfelt, 2004: Numerical simulation of
hail formation in the 28 June 1989 Bismarck thunderstorm Part II, cloud seeding results. Atmos. Res. **71**, 81-113.

Georgopoulos, P.G., and J.H. Seinfeld, 1986: Mathematical modeling of turbulent reacting plumes-General theory and model formulation. A*tmos. Envir*., **20**, 1791-1802.

Hsie, E.-Y., R.D. Farley and R. D. Orville, 1980: Numerical simulation of ice-phase convective cloud seeding. *J.Appl.Met*. **19**, 950-977.

Huston, M.W., A.G. Detwiler and F.J. Kopp, 1991: Observations and model simulations of transport and precipitation development in a seeded cumulus congestus cloud *J. Appl. Meteor*., **30**, 1389-1406.

Klemp, J.B. and R.B. Wilhelmson, 1978: The simulation of three-dimensional convective storm dynamics. *J.Atmos.Sci*. **35**, 1070-1096.

Kopp, F.J., 1988: A simulation of Alberta cumulus. *J. Appl. Meteor*., **27**, 626-641.

Lin, Y. L. Farley, R. D. and H.D. Orville, 1983: Bulk water parameterization in a cloud model. *J.Climate Appl. Met*., **22**, 1065-1092.

Smith, P.L, G. G. Myers and H.D. Orville, 1975: Radar reflectivity calculations on numerical cloud model using bulk parameterization of precipitation *J.Appl.Meteor*, **14**,1156-1165.

Orville, H. D. and F.J. Kopp, 1977: Numerical simulation of the history of a hailstorm. *J.Atmos. Sci*., **34**, 1596-1618.

Orville, H. D. and J-M.Chen, 1982: Effects of cloud seeding, latent heat of fusion and condensate loading on cloud dynamics and precipitation evolution: A numerical study. *J. Atmos. Sci*., **39**, 2807-2827.

Orville, H. D., R.D. Farley and J.H. Hirsch, 1984: Some surprising results from simulated seeding of stratiform-type clouds. *J.Climate Appl. Meteor*., **23**, 1585-1600.

Orville, H. D., W.R. Cotton, L.G. Davis, D.B. Johnson and R.M. Rauber, 1986: A \ program of Federal/state/local cooperative weather modification research: Design considerations. Part I: Hypothesis description and assessment. Final report. Department of Atmospheric Science, Colorado State University, Fort Collins, 36 pp.

Orville, H. D., F.J. Kopp, R.D. Farley, and R.B Hoffman, 1989: The numerical modeling of ice-phase cloud seeding effects in a warm-based cloud: Preliminary results. *J. Wea.Modif*., **21**,4-8.

Sekhon, R.S. and R.C. Srivastava, 1970: Snow size spectra and radar reflectivity. *J. Atmos. Sci.*, **27**, 299-307.

Smith, P.L., G.G. Myers and H.D. Orville, 1975: Radar reflectivity factor calculations on numerical cloud models using bulk parameterization of precipitation. *J. Appl. Meteor*., **14**, 1156-1165.

Spiridonov, V., and M. Curic, 2003: A three-dimensional numerical simulation of sulfate transport and redistribution *Can. J. Phys*. **81**, 1067-1094.

Spiridonov, V., and M. Curic, 2005: The relative importance of scavenging, oxidation and ice-phase processes in the production and wet deposition of sulfate. *J. Atmos. Sci.* **62**, 2118-2135.

Telenta, B., and N. Aleksic, 1988:A three-dimensional simulation of the 17 June 1978 HIPLEX case with observed ice multiplication. 2nd International Cloud Modeling Workshop, Toulouse, 8-12 August 1988. WMO/TD No. 268, 277-285.

Warburton, J.A., R.E. Elliot, W.G. Finnegan, B. Lamb, R.T. McNider and J.W. Telford, 1986: A program of federal/state/local cooperative weather modification research: Design considerations. Part II: Transport and dispersion of seeding materials. Final Report Department of Atmospheric Science, Colorado State University, Fort, 75 Collins pp.

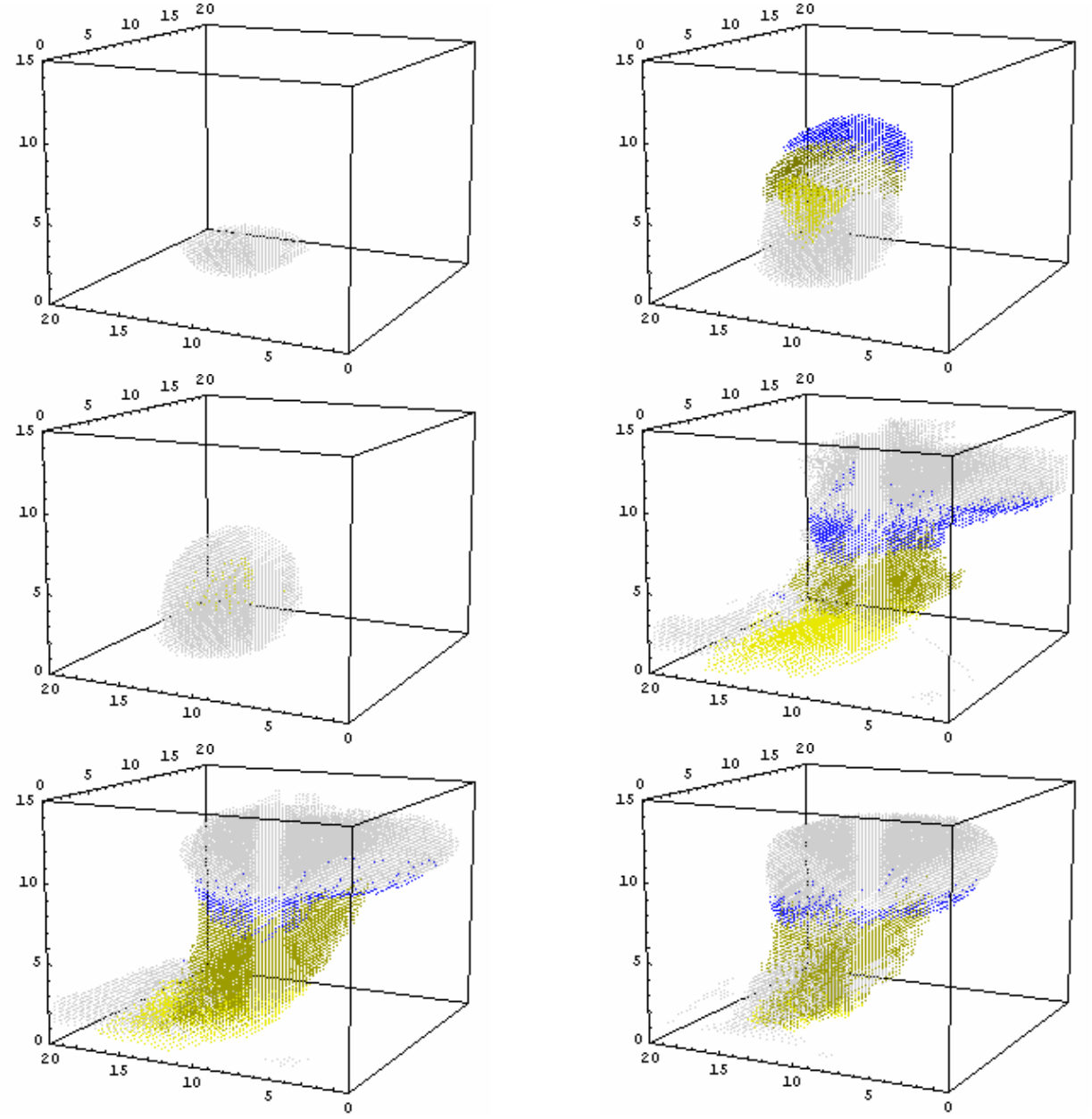

**Figure 2a.** Model simulated three-dimensional surfaces of the given mass mixing ratios (g/kg) at 10 min time intervals, starting at 10 min of simulation time. Gray plots represent total non-precipitating water (cloud water +cloud ice) with the cloud outline of 0.01 g $kg^{-1}$.The precipitating fields are blue, brown and yellow representing the mixing ratios of snow, hail and rain ≥0.1 g $kg^{-1}$. The domain dimensions are 20x20x15$km^3$.

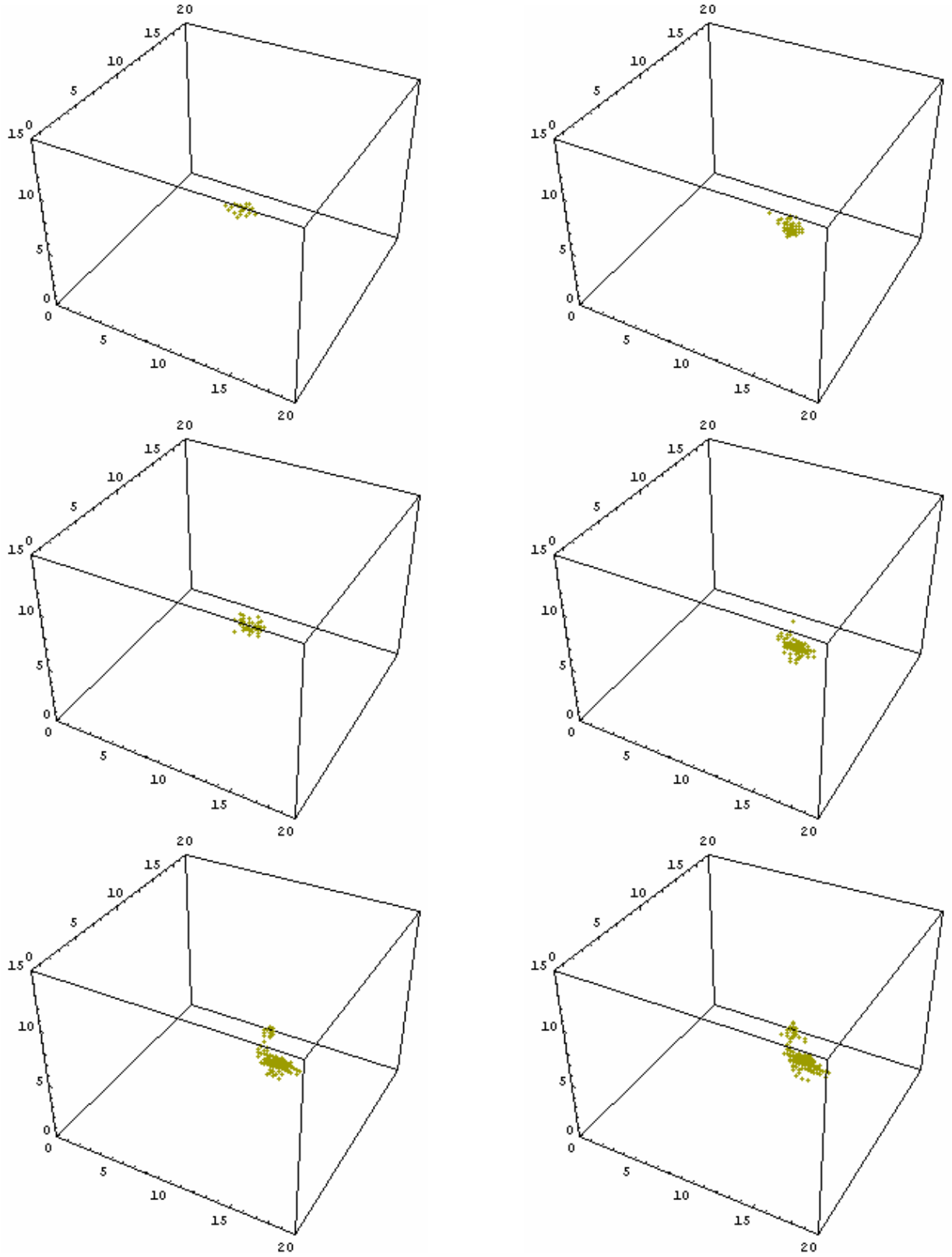


**Figure 2b.**Three-dimensional depictions of the AgI field viewed from SSE at 5 min intervals starting at 23.3 min of simulation time. The 0.1 μg $kg^{-1}$ surface is indicated in these plots.

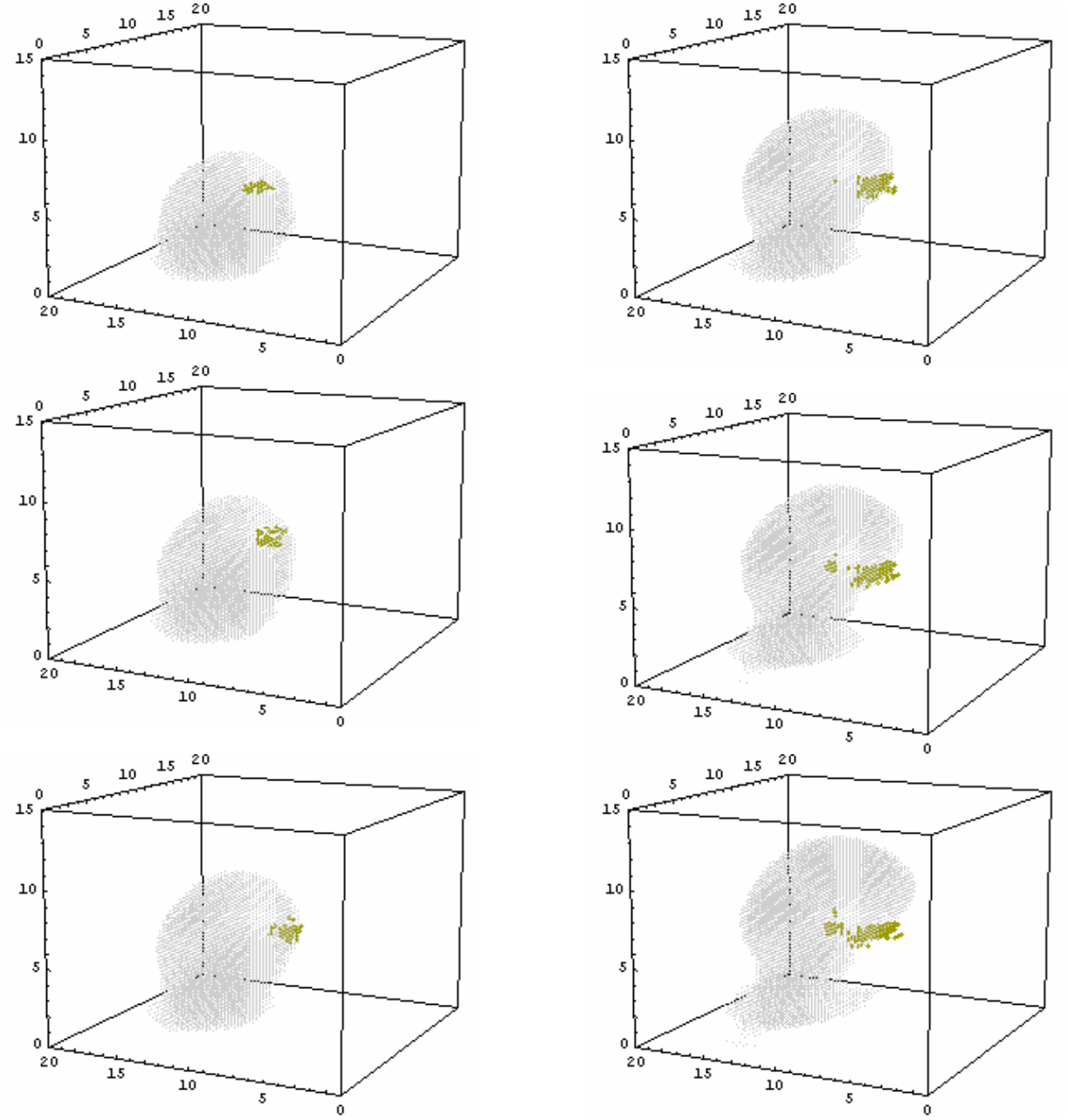

**Figure 2c.** Three-dimensional depictions of (cloud water + AgI field) viewed from SE at 5 min intervals starting at 23.3 min of simulation time. The cloud outline is indicated by 0.001 g $kg^{-1}$. The 0.1 µg $kg^{-1}$ surface is indicated for AgI field in these panels. .

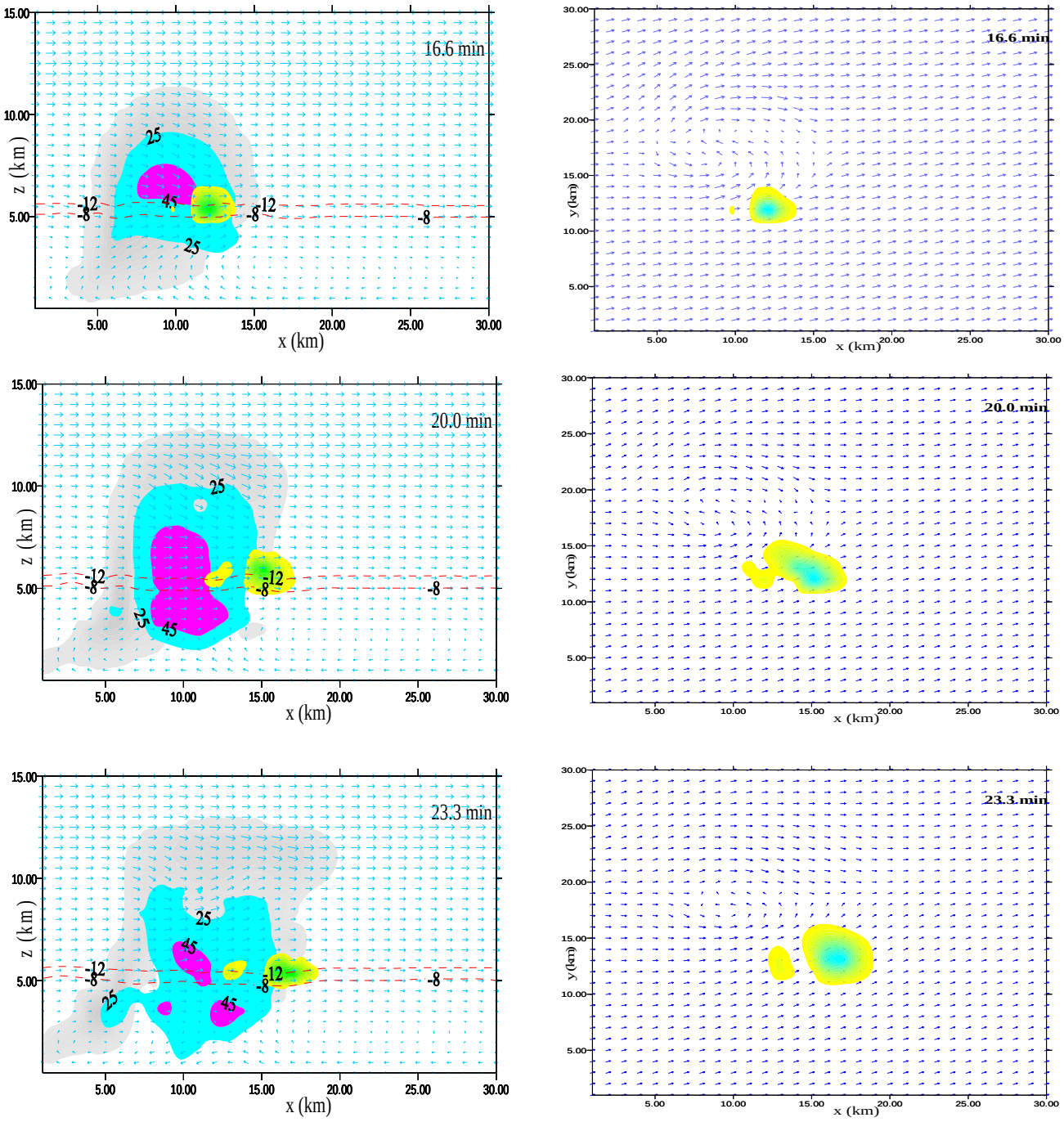


**Figure 3. a)** Time evolution of AgI (μg kg$^{-1}$) in the x-z plane at y = 15 km (left panel) for Negotino storm on May 18, 2003, in 16.6, 20.0, 23.3 and 26.6 min of simulation time. The domain dimensions are 30x30x15km$^3$. Cloud surfaces (gray) with cloud outline contour of 0.01 g kg$^{-1}$. AgI fields are (green and yellow), while the reflectivity contours are represented with light green and violet color. **b)** Time evolution of AgI (μg kg$^{-1}$) in the x-y plane at z = 5.5 km in 16.6, 20.0, 23.3 and 26.6 min of simulation time. The domain dimensions are 30x30x15km$^3$ (right panel).

**Table 1.** Maximum percentage values of each sink term representing the five nucleation mechanisms (Brownian collection and inertial impact due to cloud droplets and raindrops and deposition nucleation) and the total rainfall and hailfall accumulated on the ground expressed in ($kg/m^2$) and (%), in different time frequency of seeding.

| Run | Time frequency of seeding (min) | Brownian collection cloud drops | Inertial impact cloud drops | Brownian collection raindrops | Inertial impact raindrops | Deposition (sorption) | Rainfall ($kg/m^2$) | Hailfall ($kg/m^2$) | Rainfall (%) | Hailfall (%) |
|---|---|---|---|---|---|---|---|---|---|---|
| Base run A | Unseeded | | | | | | **150.51** | **18.18** | | |
| A0 | 0 (20min) | 0.143 | 0.014 | 0.004 | 0.048 | 87.6 | 159.89 | 18.12 | 6.23 | 0.33 |
| A1 | 1 (20,21,22) | 0.482 | 0.031 | 0.003 | 0.053 | 78.1 | 167.32 | 17.23 | 11.16 | 5.22 |
| A2 | 2 (20,22,24) | 0.645 | 0.026 | 0.003 | 0.060 | 84.6 | 174.44 | 16.76 | 15.89 | 7.81 |
| A3 | 3 (20,23,26) | 0.560 | 0.044 | 0.005 | 0.077 | 95.2 | 176.01 | 16.22 | 16.94 | 10.78 |
| A4 | 4(20,24,28) | 0.793 | 0.052 | 0.006 | 0.071 | 91.4 | 189.333 | 16.36 | 25.79 | 10.01 |
| A5 | 5 (20,25,30) | 0.711 | 0.058 | 0.004 | 0.083 | 90.3 | 182.87 | 16.37 | 21.50 | 9.95 |
| A6 | 6(20,26,32) | 0.538 | 0.045 | 0.002 | 0.074 | 89.7 | 177.29 | 16.18 | 17.79 | 11.01 |
| A7 | 7 (20,27,34) | 0.469 | 0.037 | 0.000 | 0.062 | 84.8 | 170.48 | 16.98 | 13.26 | 6.60 |
| A8 | 8 (20,28,36) | 0.333 | 0.027 | 0.000 | 0.054 | 84.4 | 163.60 | 16.55 | 8.69 | 8.96 |
| A9 | 9 (20,29,38) | 0.265 | 0.034 | 0.000 | 0.043 | 83.0 | 156.20 | 16.73 | 10.42 | 7.97 |
| A10 | 10 (20,30,40) | 0.201 | 0.029 | 0.000 | 0.048 | 78.5 | 155.18 | 17.00 | 9.74 | 6.49 |

**Table 2.** Model sensitivity experiments to the physical and AgI dispersion processes. The parameters listed in columns (5-12), represent the maximum calculated values during simulation time of puff concentration ($g/m^3$), spread of the puff diameter (m), vertical extent of puff (m) and AgI mixing ratio together with the total accumulated rainfall and hailfall in ($kg/m^2$ and %) on the ground, using different initial amount of seeding (g/m), seeding time (min), seeding height (km) and seeding distance (km), given in columns 1-4 in the same Table.

| RUN | Seeding amount (g/m) | Initial seeding time (min) | Seeding height (km) | Seeding distance X,Y (km) | QPUFF Conc. of puff ($g/m^3$) | DPUF Spread of the puff diam. (m) | ZPUF Vert. extent of puff diam. (m) | RN AgI mixing ratio (g/kg) | Total acc. rainfall at the ground ($kg/m^2$) | Total acc. hailfall at the ground ($kg/m^2$) | Rainfall (%) | Hailfall (%) |
|---|---|---|---|---|---|---|---|---|---|---|---|---|
| Base run B | / | | | | Unseeded case | / | / | / | 150.51 | 18.18 | | |
| B1 | 0.1 | 15.0 | 5.5 | 11, 11 | $0.52x10^{-5}$ | 87.6 | 6967 | $0.72x10^{-9}$ | 155.04 | 18.12 | 3.00 | 0.33 |
| **B2** | **0.4** | **16.6** | **5.5** | **10, 10** | $0.20x10^{-4}$ | **79** | **6992** | $1.71x10^{-9}$ | **189.33** | **16.36** | **25.79** | **10.01** |
| B3 | 0.6 | 15.0 | 5.0 | 10.5, 10.5 | $0.31x10^{-4}$ | 77.5 | 7023 | $2.03x10^{-9}$ | 182.13 | 16.51 | 21.00 | 9.18 |
| B4 | 0.8 | 16.6 | 6.0 | 11, 11 | $0.40x10^{-4}$ | 77 | 6889 | $2.74x10^{-9}$ | 178.13 | 16.77 | 18.35 | 7.75 |
| B5 | 1.0 | 16.6 | 4.5 | 9.5, 9.5 | $0.56x10^{-4}$ | 75 | 6863 | $3.90x10^{-9}$ | 169.23 | 17.28 | 12.43 | 4.95 |
| B6 | 1.5 | 16.6 | 5.0 | 10,10 | $0.79x10^{-4}$ | 77.5 | 7016 | $6.45x10^{-9}$ | 165.84 | 17.16 | 10.18 | 5.61 |
| B7 | 2.0 | 16.6 | 5.5 | 10,10 | $0.98x10^{-4}$ | 78.5 | 6751 | $8.83x10^{-9}$ | 158.08 | 17.25 | 5.03 | 5.11 |

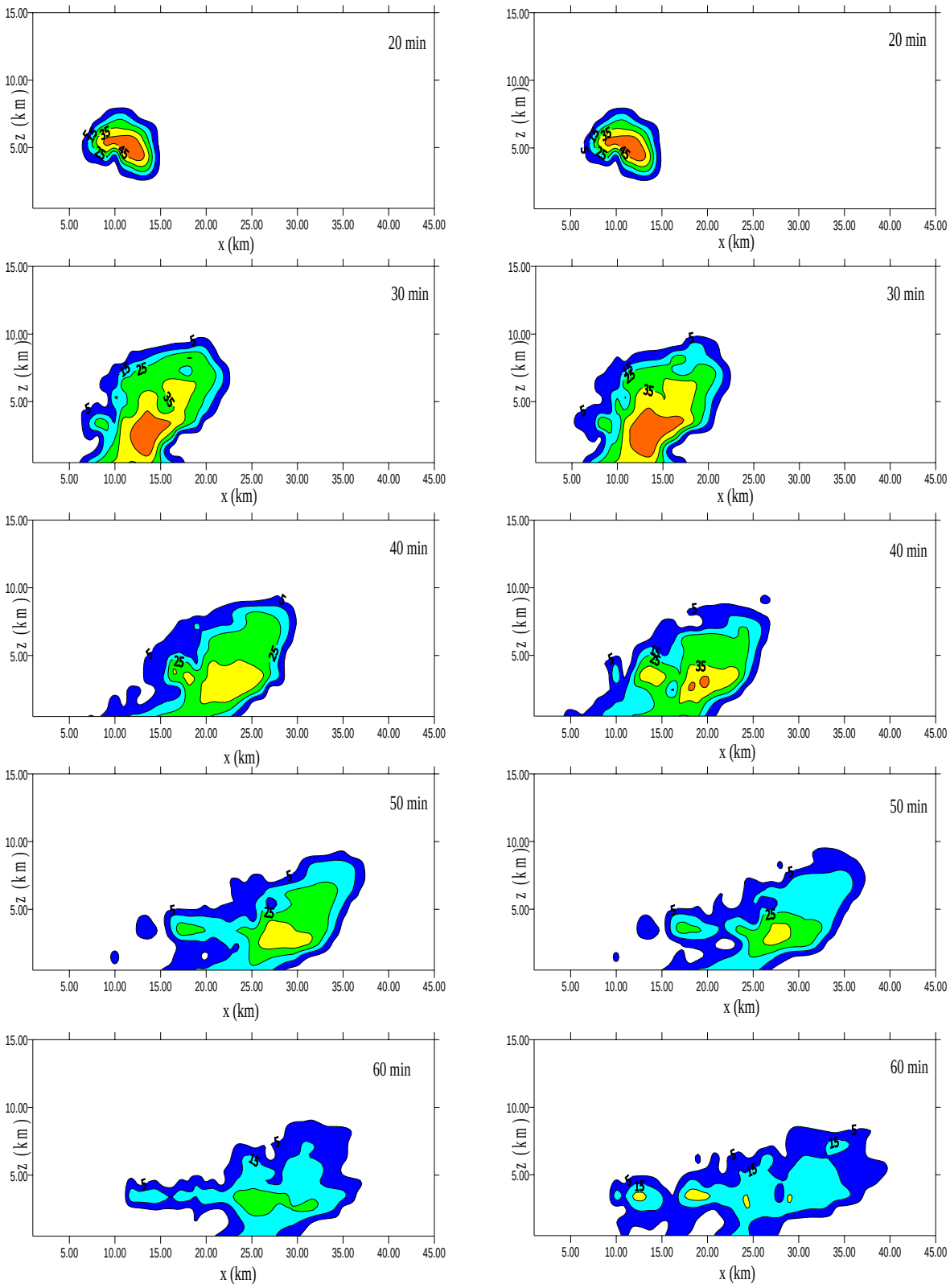


**Figure 4.** The vertical x-z cross sections of reflectivity patterns of the unseeded (l.s. panels) and seeded cloud (r.h. panels) at 20,30,40,50 and 60 min.of the simulation time running a two-dimensional version of the model with dimensions of 45x15km$^2$.